23

Sensorless V/f Control of Permanent Magnet Synchronous Motors

Daniel Montesinos-Miracle[1], P. D. Chandana Perera[2], Samuel Galceran-Arellano[1] and Frede Blaabjerg[3]
[1]*Centre d'Innovació Tecnològica en Convertidors Estàtics i Accionaments, Departament d'Enginyeria Elèctrica, Universitat Politècnica de Catalunya*
[2]*Department of Electrical and Information Engineering, Faculty of Engineering, University of Ruhuna*
[3]*Institute of Energy Technology, Aalborg University*
[1]*Spain*
[2]*Sri Lanka*
[3]*Denmark*

1. Introduction

The increasing energy cost demands for more efficient motion control systems in domestic and industrial applications. Power electronics and control can contribute to increase the efficiency of present systems, but it can also be dealt with new efficient solutions for old applications.

Instead of using constant speed using variable speed drives in motion control applications the efficiency of the systems can be increased. The most common control methods used in drives are V/f control, vector control and direct torque control (DTC) [1]. In continuous running applications, a small increase in efficiency means a huge energy savings per year. These continuous running applications are mainly pumps, fans and compressors for heating, ventilating and air conditioning (HVAC) applications. In these applications where high dynamics are not required, a simple digital implementation of V/f control can be used instead of more complex vector or DTC with the same performance [2, 3].

The workhorse for these applications has been the induction motor for years. The induction motor is a well known motor, a cheap motor, and does not require position sensor to implement a low-cost control for this kind of applications.

But efficiency can be improved if the induction motor is substituted by a permanent magnet synchronous motor (PMSM) [4]. However, in permanent magnet synchronous motors, the stator currents have to be synchronized with the rotor permanent magnet in order to produce the required torque and not to lose synchronization. For this purpose a rotor position sensor is required. The need of a rotor position sensor increases the cost and reduces the reliability. Self synchronization can be achieved using damper windings [5], but due to cost, efficiency and high-cost, they are generally not implemented in PMSMs [6].

Therefore, it is necessary to develop new control strategies for PMSMs to avoid the use of the rotor position sensor. Because HVAC applications do not demand for a high

performance control, the V/f control strategy is suitable for these drives. However, even using a V/f control strategy for permanent magnet synchronous motors, there is a need in synchronization for stator currents with the rotor magnet position.
This chapter present a sensorless V/f control for permanent magnet synchronous motors.

2. Park equations of permanent magnet synchronous motors

The Park transformation is useful when modeling a PMSM, since there is no angle dependent terms appear in equations, providing easy analysis of the system [7].
With the electrical equations in Park variables, it is easy to obtain an expression for the motor generated torque as a function of electrical variables. This produced mechanical torque links the electrical world with the mechanical world, and completes the model of the system. The model equations of the permanent magnet synchronous motor in Park variables are:

$$\dot{i}_{ds}^{r} = -\frac{R_s}{L_d} i_{ds}^{r} + \omega_r \frac{L_q}{L_d} i_{qs}^{r} + \frac{v_{ds}^{r}}{L_d} \tag{1.1}$$

$$\dot{i}_{qs}^{r} = -\frac{R_s}{L_q} i_{qs}^{r} - \omega_r \frac{L_d}{L_q} i_{ds}^{r} - \frac{\lambda_m}{L_q} \omega_r + \frac{v_{qs}^{r}}{L_q} \tag{1.2}$$

$$\dot{\omega}_r = \frac{3}{2}\left(\frac{n}{2}\right)^2 \frac{1}{J_m} \lambda_m i_{qs}^{r} + \frac{3}{2}\left(\frac{n}{2}\right)^2 \frac{1}{J} \left(L_d - L_q\right) i_{ds}^{r} i_{qs}^{r} - \frac{B_m}{J_m} \omega_r - \frac{n}{2J} T_l \tag{1.3}$$

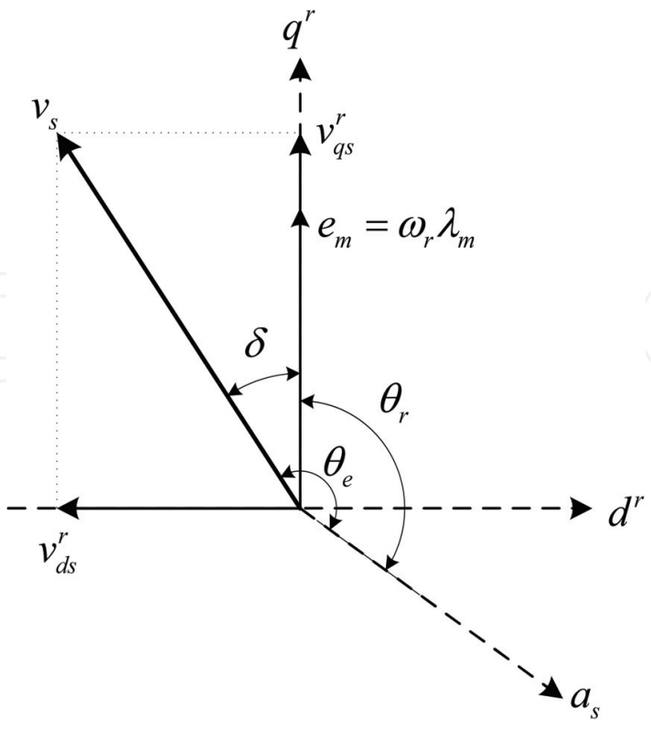

Fig. 1.1. Load angle

Sometimes, it is useful to define a new variable called load angle [8]. The load angle is the angle between the stator electrical applied voltage and the *emf* generated by rotor magnets when rotating, as can be seen in Figure 1.1. With this new equation, the system equations in state space variables are defined as

$$\dot{i}_{ds}^{r} = -\frac{R_s}{L_d} i_{ds}^{r} + \omega_r \frac{L_q}{L_d} i_{qs}^{r} - \frac{v_s \sin\delta}{L_d} \tag{1.4}$$

$$\dot{i}_{qs}^{r} = -\frac{R_s}{L_q} i_{qs}^{r} - \omega_r \frac{L_d}{L_q} i_{ds}^{r} - \frac{\lambda_m}{L_q}\omega_r + \frac{v_s \cos\delta}{L_q} \tag{1.5}$$

$$\dot{\omega}_r = \frac{3}{2}\left(\frac{n}{2}\right)^2 \frac{1}{J_m}\lambda_m i_{qs}^{r} + \frac{3}{2}\left(\frac{n}{2}\right)^2 \frac{1}{J}\left(L_d - L_q\right) i_{ds}^{r} i_{qs}^{r} - \frac{B_m}{J_m}\omega_r - \frac{n}{2J}T_l \tag{1.6}$$

$$\dot{\delta} = \omega_e - \omega_r \tag{1.7}$$

The above equations are the state space model, but this model contains non-linear terms. To analyze the stability of the system, a linear model must be obtained.

3. Stability analysis

The non-linear model can be linearized by substituting each variable as [8]

$$x_i = X_i + \Delta x_i \tag{1.8}$$

where x_i is the variable, X_i is the steady state value, and Δx_i is a perturbation from the steady state value. Then, the linearized system is

$$\Delta\dot{\mathbf{x}} = \mathbf{A}\left(\mathbf{X}\right)\Delta\mathbf{x} + \mathbf{B}\left(\mathbf{X}\right)\Delta\mathbf{u} \tag{1.9}$$

Applying this linearization technique to the state space model of the permanent magnet synchronous motor, the linearized model is obtained as

$$\begin{Bmatrix} \Delta\dot{i}_{ds}^{r} \\ \Delta\dot{i}_{qs}^{r} \\ \Delta\dot{\omega}_r \\ \Delta\dot{\delta} \end{Bmatrix} = \begin{pmatrix} -\frac{R_s}{L_d} & \frac{L_q\omega_{r0}}{L_d} & \frac{L_q I_{qs}^{r}}{L_d} & -\frac{V_s\cos\delta_0}{L_d} \\ -\frac{L_d\omega_{r0}}{L_q} & -\frac{R_s}{L_q} & -\frac{1}{L_q}\left(L_d I_{ds}^{r} + \lambda_m\right) & -\frac{V_s\sin\delta_0}{L_q} \\ \frac{3}{2}\left(\frac{n}{2}\right)^2\frac{1}{J_m}\left(L_d - L_q\right)I_{qs}^{r} & \frac{3}{2}\left(\frac{n}{2}\right)^2\frac{1}{J_m}\left(\lambda_m + \left(L_d - L_q\right)I_{ds}^{r}\right) & -\frac{B_m}{J_m} & 0 \\ 0 & 0 & -1 & 0 \end{pmatrix} \begin{Bmatrix} \Delta i_{ds}^{r} \\ \Delta i_{qs}^{r} \\ \Delta\omega_r \\ \Delta\delta \end{Bmatrix} + \begin{pmatrix} -\frac{\sin\delta_0}{L_d} & 0 & 0 \\ \frac{\cos\delta_0}{L_q} & 0 & 0 \\ 0 & 0 & -\frac{n}{2J_m} \\ 0 & 1 & 0 \end{pmatrix} \begin{Bmatrix} \Delta v_s \\ \Delta\omega_e \\ \Delta T_l \end{Bmatrix} \tag{1.10}$$

3.1. V/f open loop control

When the motor is operated at open loop V/f control, the applied voltage and frequency are constant, that is

$$\Delta v_s = 0 \tag{1.11}$$

$$\Delta \omega_e = 0 \tag{1.12}$$

The stability of the system is determined by the eigenvalues of the state matrix **A**(**X**). In open loop V/f control strategy with no-load, the motor produces no torque. Then, $I^r_{qs} = 0$. In order to minimize the losses, I^r_{ds} is also 0. In this case, the applied voltage must only compensate the *emf* in the q axis, $V_s = \omega_r \lambda_m = V^r_{qs}$ and $V^r_{ds} = 0$. Substituting this steady state conditions in the state matrix **A**(**X**) it is possible to obtain the stability characteristic of the system. Figure 1.2 shows the root locus diagram of the permanent magnet synchronous motor in an open loop V/f control at no-load as a function of stator frequency ω_e. For this figure the motor data can be found in Appendix A.

As seen in Figure 1.2, the motor becomes unstable above 100 Hz operation, i. e. half of the rated frequency. The most left poles are the named stator poles, and represent the fast electrical stator dynamics [9, 8]. The most right poles are named the rotor poles, and represent the slow mechanical dynamics. A poor coupling between the rotor and stator poles causes this instability [10, 11].

Figure 1.3 shows the dominant poles at different load levels. As seen, the stability characteristic is not modified with the load level.

Figure 1.4 shows this instability in a real system. As seen, at low frequency, the motor is stable (Figure 1.4(a)), but when increasing the frequency the motor becomes unstable (Figures 1.4(b) and 1.4(c)).

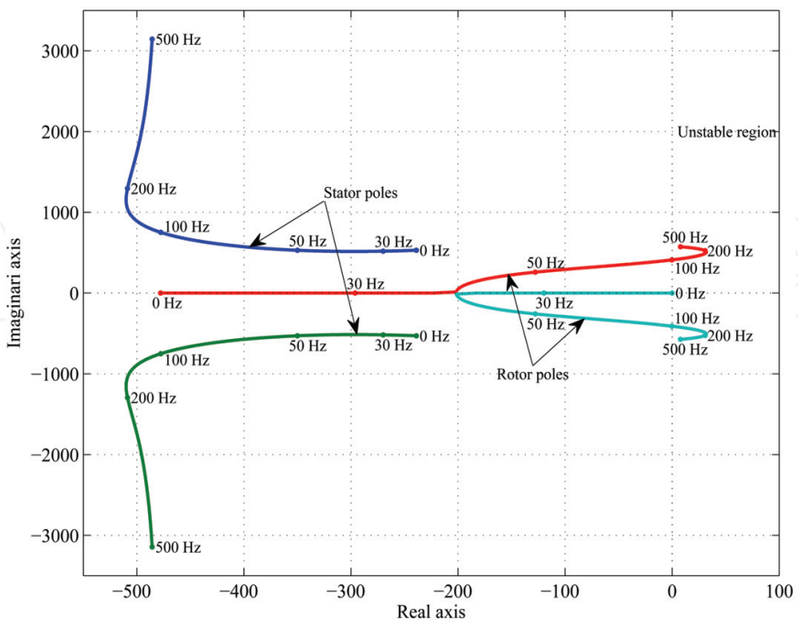

Fig. 1.2. Root locus of the permanent magnet synchronous motor operating at no-load in an open loop V/f control strategy

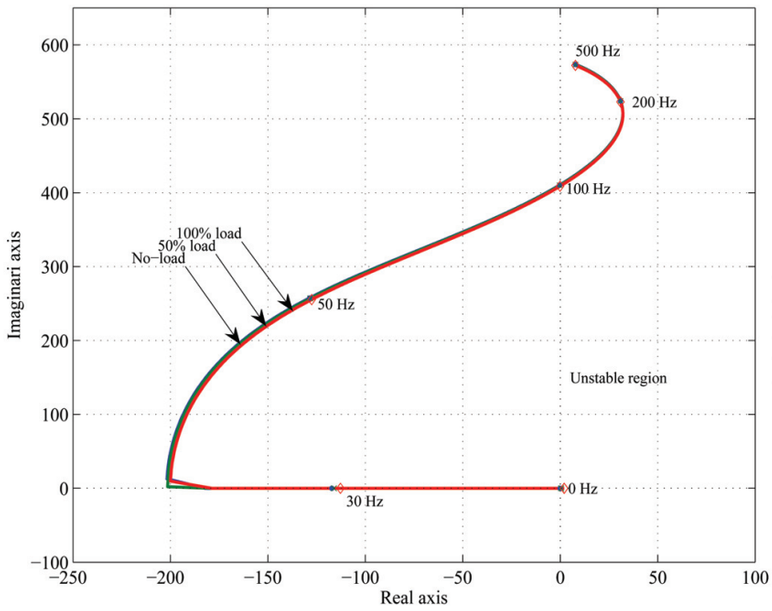

Fig. 1.3. Root locus of the permanent magnet synchronous motor operating at different load levels in an open loop V/f strategy

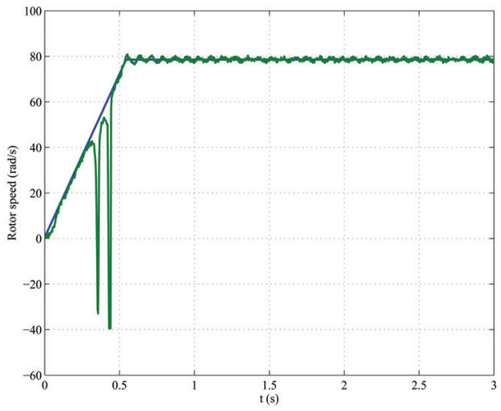

(a) Rotor speed at 50Hz stator frequency

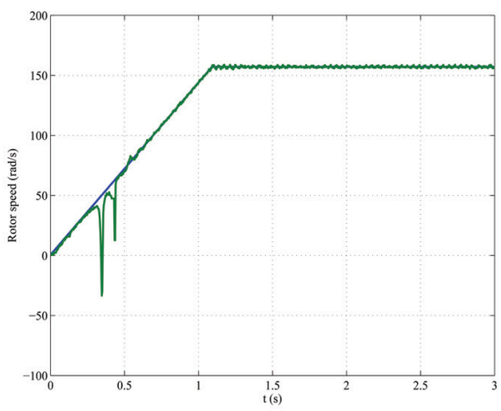

(b) Rotor speed at 100 Hz stator frequency

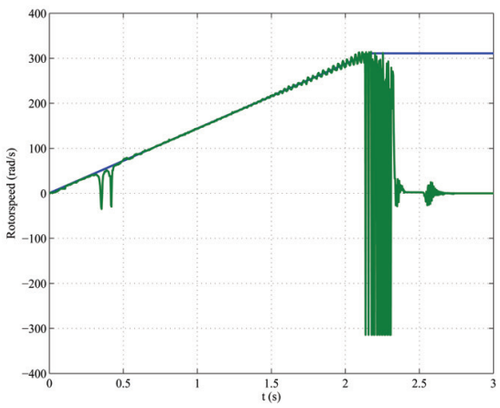

(c) Rotor speed at 200 Hz stator frequency

Fig. 1.4. Rotor speed at different stator frequencies in the open loop V/f control strategy

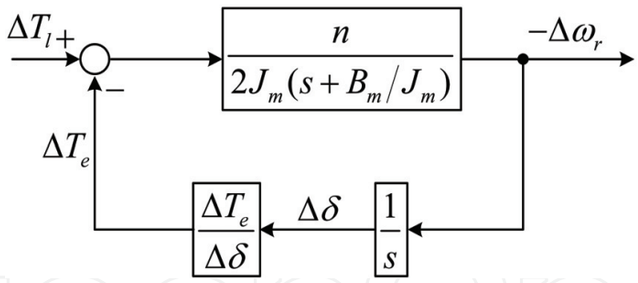

Fig. 1.5. Block diagram of the small signal model operating at V/f open loop control strategy

4. Stabilization of the V/f control in permanent magnet synchronous motor

The open loop V/f control does not assure the synchronization between stator currents and rotor position needed. If this synchronization is lost, the motor becomes unstable above a rotating frequency, as seen in section 1.3.
In order to operate the motor in a V/f control, a synchronization method is needed. The method proposed in this section is based on the stabilization of the operation of the permanent magnet synchronous motor in a V/f control strategy.

4.1 Small signal model of the permanent magnet synchronous motor

Assuming that the motor is operating in open loop V/f control, from the linearized model, the block diagram of Figure 1.5 can be obtained. The expression of $\frac{\Delta T_e}{\Delta\delta}$ is

$$\frac{\Delta T_e}{\Delta\delta}=\frac{3}{2}\frac{n}{2}\lambda_m\frac{\left(I_{ds}^r+\frac{\lambda_m}{L_d}\right)s^2+\frac{R_s}{L_d}\left(\frac{\lambda_m}{L_d}-2I_{ds}^r\right)s+\omega_{r0}^2\left(\frac{\lambda_m}{L_d}+I_{ds}^r\right)+\frac{R_s^2}{L_d^2}I_{ds}^r}{s^2+\frac{2R_s}{L_d}s+\frac{R_s^2}{L_d^2}+\omega_{r0}^2} \tag{1.13}$$

In Figure 1.5, it can be seen that small load torque perturbations produce small rotating speed perturbations, through mechanical dynamics, that produce small perturbations of the load angle, that produce small produced torque perturbations.
It can be observed in equation (1.13) that, motor stability is not an explicit function of the torque in steady state, but, for a given voltage value, the current I_{ds}^r and therefore, coefficients in (1.13), are a function of torque. It must also be noted that, combinations of voltage and torque that gives equal values of I_{ds}^r, will have the same stability characteristic. In control methods that impose I_{ds}^r= 0, all the operating points will have the same stability characteristics [12].
From this model a simplification can be done supposing that the perturbations of T_e are linear with Δδ as [10],

$$\Delta T_e=K_e\Delta\delta \tag{1.14}$$

where K_e is the electromechanic spring constant. The electromagnetic torque in steady state T_{e0} is an expression of V_s, ω_r and δ_0. Now, the characteristic equation of the system operating in open loop is

$$1+\frac{n}{2J_m\left(s+\frac{B_m}{J_m}\right)}\frac{K_e}{s}=0 \tag{1.15}$$

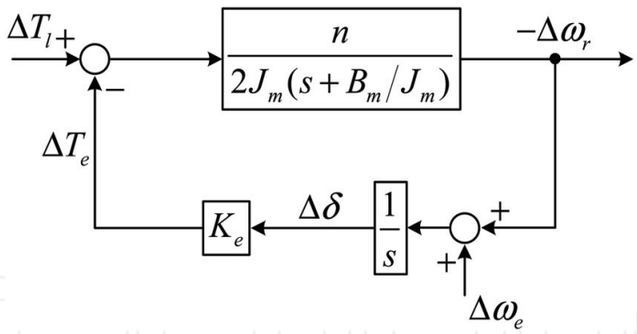

Fig. 1.6. Block diagram of the simplified small signal model operating at V/f control strategy

But looking at the model in (1.10), the perturbation of the load angle Δδ can be expressed as

$$\Delta\delta = \int (\Delta\omega_e - \Delta\omega_r)\, dt \tag{1.16}$$

and the model of Figure 1.6 can be obtained.

The instability of the permanent magnet synchronous motor described in section 1.3 is due to the low coupling between the electrical and mechanical modes. This instability shows a relatively small positive value of the dominant poles of the system. Therefore, a small damping must be added to the system to stabilize it [12]. In order to add this damping, it is only necessary to add to the torque a component proportional to the perturbation speed as

$$\Delta\omega_e = -K_v \frac{d\Delta\omega_r}{dt} \tag{1.17}$$

as seen in Figure 1.7. Now, the characteristic equation is

$$s^2 + \frac{2B_m + n + K_e K_v}{2J_m} s + \frac{n}{2J_m} K_e = 0 \tag{1.18}$$

and the stability characteristic of the system can be determined by K_v. This stabilization can be implemented measuring speed and extracting the perturbation, but then, a speed sensor is needed.

4.2 Stabilizing using power perturbations

Power perturbations can also be used to modulate the excitation frequency in order to add damping to the system and stabilize it. The power can be expressed as a steady state value plus a perturbation as

$$p_e = P_e + \Delta p_e = P_p + \frac{dW_e m}{dt} + \left(\frac{2}{n}\right)^2 \frac{J_m}{2} \frac{d}{dt}\omega_r^2 + \left(\frac{2}{n}\right)^2 B_m \omega_r^2 + \frac{2}{n}\omega_r T_l \tag{1.19}$$

where the first term are the loses and for small perturbations can be considered constant. The second term is the variation of the stored magnetic energy, and, however it is not constant, has a constant average value in an electrical rotation. Then, the power perturbations can be expressed as

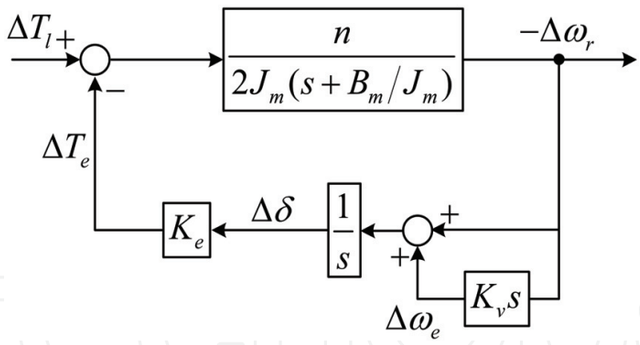

Fig. 1.7. Block diagram of the small signal model when the applied frequency is modulated with rotor speed perturbations

$$\Delta p_e = \left(\frac{2}{n}\right)^2 J_m \omega_{r0} \frac{d}{dt}\Delta\omega_r + 2\left(\frac{2}{n}\right)^2 B_m \omega_{r0}\Delta\omega_r + \frac{2}{n} T_{l0}\Delta\omega_r \tag{1.20}$$

Looking at equation (1.20) and at Figure 1.6, the excitation frequency can be modulated proportional to input power perturbations as

$$\begin{aligned}\Delta\omega_e &= -K_p \Delta p_e = \\ &- K_p \left(\left(\frac{2}{n}\right)^2 J_m \omega_{r0} \frac{d}{dt}\left(-\Delta\omega_r\right) + 2\left(\frac{2}{n}\right)^2 B_m \omega_{r0}\left(-\Delta\omega_r\right) + \frac{2}{n} T_{l0}\left(-\Delta\omega_r\right) \right)\end{aligned} \tag{1.21}$$

and the block diagram of Figure 1.8 can be obtained. With this modulation technique, the characteristic equation of the system is

$$s^2 + \left(\frac{B_m}{J_m} + \frac{2K_e\omega_{r0}K_p}{n}\right) s + \frac{K_e}{2J_m}\left(n + 4\frac{2}{n} B_m K_p \omega_{r0} + 2T_{l0}K_p\right) = 0 \tag{1.22}$$

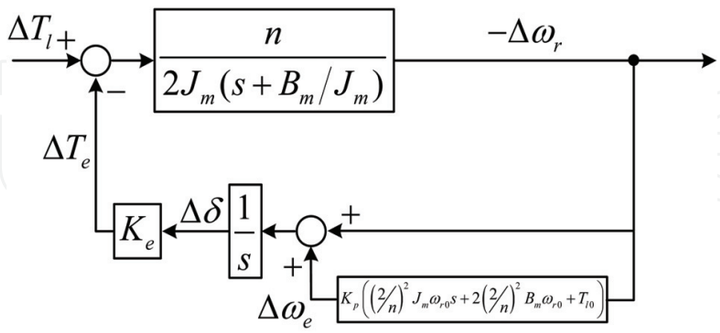

Fig. 1.8. Block diagram of the simplified smal signal model operating at V/f control where the applied frequency is modulated with input power perturbations

and the poles of the system are

$$s = -\left(\frac{B_m}{2J_m} + \frac{K_e\omega_{r0}K_p}{n}\right) \pm \sqrt{\left(\frac{B_m}{2J_m} + \frac{K_e\omega_{r0}K_p}{n}\right)^2 - \frac{K_e}{2J_m}\left(n + 4\frac{2}{n} B_m K_p \omega_{r0} + 2T_{l0}K_p\right)} \tag{1.23}$$

It can be seen that the damping of the system can be determined by the value of K_p in a steady state operation point. But, observing equation (1.20), it is possible to see that imposing a constant value of K_p, it is not possible to fix the poles of the system in the whole speed operating range. It is possible to almost fix the poles of the system not fixing K_p, but fixing the product $K_p\omega_{r0} = C_p$.

The frequency modulation can also be done using the perturbations of the DC link current [10]. Supposing that the DC link voltage is constant, power can be expressed as

$$p_e = P_e + \Delta p_e = V_{DC}\left(I_{DC} + \Delta i_{DC}\right) = P_p + \frac{dW_e m}{dt} + \left(\frac{2}{n}\right)^2 \frac{J_m}{2}\frac{d}{dt}\omega_r^2 + \left(\frac{2}{n}\right)^2 B_m\omega_r^2 + \frac{2}{n}\omega_r T_l \quad (1.24)$$

if power at transistor level are not considered. Then, the modulation of the exciting frequency can be done as

$$\Delta\omega_e = -K_i\Delta i_{DC} = \frac{1}{V_{DC}}\left(\left(\frac{2}{n}\right)^2 J_m\omega_{r0}\frac{d}{dt}\left(-\Delta\omega_r\right) + 2\left(\frac{2}{n}\right)^2 B_m\omega_{r0}\left(-\Delta\omega_r\right) + \frac{2}{n}T_{l0}\left(-\Delta\omega_r\right)\right) \quad (1.25)$$

But, must be noted that

$$K_i = K_p V_{DC} \quad (1.26)$$

giving the same stability characteristics using input power perturbations and DC link current perturbations.

4.3 Stability verification

In the model expressed in (1.2), a new equation that describes the modulation of the excitation frequency must be added as

$$\Delta\omega_e = -K_p\Delta p_e \quad (1.27)$$

where input power perturbations are computed using a first order filter as

$$\Delta p_e = \frac{s}{s + \frac{1}{\tau_h}} p_e \quad (1.28)$$

where τ_h is high-pass filter time constant. Then, the fifth differential equation is

$$\Delta\dot{\omega}_e + \frac{\Delta\omega_e}{\tau_h} = -K_p\dot{p}_e \quad (1.29)$$

The input power can be calculated using the Park's voltages and currents as

$$p_e = \frac{2}{3}\left(v_{ds}^r i_{ds}^r + v_{qs}^r i_{qs}^r\right) \quad (1.30)$$

Supposing that the voltage is constant, i.e. no perturbation is applied, the time derivative of the power can be expressed as

$$\dot{p}_e = \frac{2}{3}V_s\left(-\dot{i}^r_{ds}\sin\delta + \dot{i}^r_{qs}\cos\delta - \left(i^r_{ds}\cos\delta + i^r_{qs}\sin\delta\right)\dot{\delta}\right) \tag{1.31}$$

To obtain the fifth system equation, equation (1.31) must be substituted in (1.29). Substituting time derivative expressions of currents and load angle, one can obtain the fifth differential equation as

$$\begin{aligned}\Delta\dot{\omega}_e = &\frac{3}{2}K_pV_s\left(\frac{\omega_r L_d\cos\delta}{L_q} - \frac{R_s\sin\delta}{L_d} + (\omega_e-\omega_r)\cos\delta\right)i^r_{ds}\\ &+\frac{3}{2}K_pV_s\left(\frac{\omega_r L_q\sin\delta}{L_d} + \frac{R_s\cos\delta}{L_q} + (\omega_e-\omega_r)\sin\delta\right)i^r_{qs}\\ &+\frac{3}{2}K_pV_s\frac{\lambda_m\cos\delta}{L_q}\omega_r\\ &-\frac{3}{2}K_pV_s\left(\frac{V_s\sin^2\delta}{L_d} - \frac{V_s\cos^2\delta}{L_q}\right)\\ &-\frac{1}{\tau_h}\Delta\omega_e\end{aligned} \tag{1.32}$$

Linearizing the new system, one can obtain the stability characteristics of the system with the modulation of the frequency using input power perturbations. The linearized system can be seen in Appendix B. Figure 1.9 shows the root locus as a function of K_p. As seen in Figure 1.9, the motor is stable for a range of values of K_p. The value of the K_p determines, as previously seen, the stability characteristics of the system. In this case, the cut-off frequency of the high-pass filter used to extract the input power perturbations is 2.5 Hz. The time constant τ_h is 0.0637 s. That locates the fifth pole of the system at s =-16. As seen in Figure 1.9, the rotor poles moves from the unstable region to stable region as K_p increases, but the stator poles moves from stable region to unstable region, giving the limits of the constant K_p.

As said before, in order to maintain the stability characteristics of the motor in the whole frequency range, the product $C_p = K_p\omega_{r0}$ is maintained constant. In this case, C_p =12.5664, giving a value of K_p =0.01 at rated speed.

The root locus of the motor as a function of excitation frequency can be seen in Figure 1.10. As seen in Figure 1.10 the poles of the system remains now in the stable region in the whole frequency range. It can also be seen in Figure 1.10 that the stability characteristics of the system is almost constant for frequencies above 100 Hz. This is because of the constant $C_p = K_p\omega_{r0}$ product.

5. Implementation of the stabilized V/f control

As seen in Figure 1.11, the implementation of the V/f control of PMSM with stabilization loop has two main parts. First the computation of power perturbations, and second, the computation of the voltage applied to the motor.

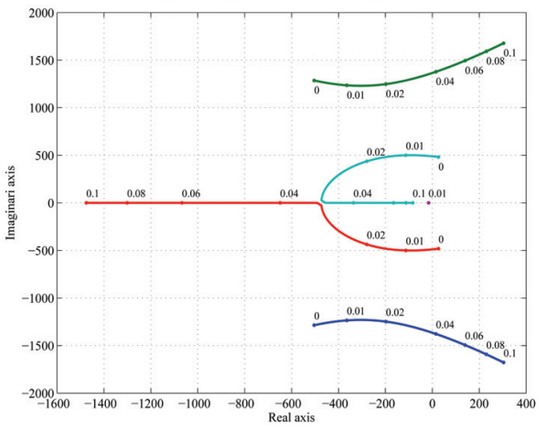

(a) Root locus of the system as a function of K_p operating the motor at no-load and rated speed

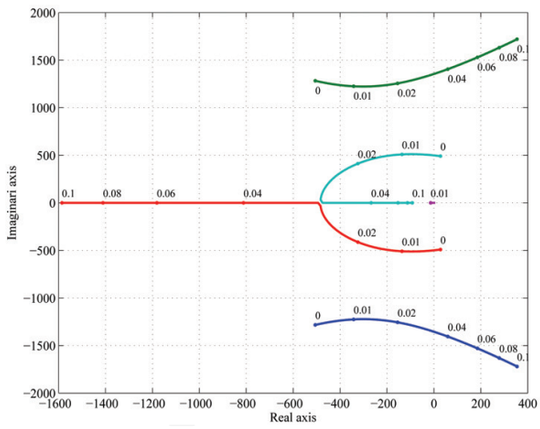

(b) Root locus of the system as a function of K_p operating the motor at full-load and rated speed

Fig. 1.9. Root locus of the stabilized motor as a function of K_p

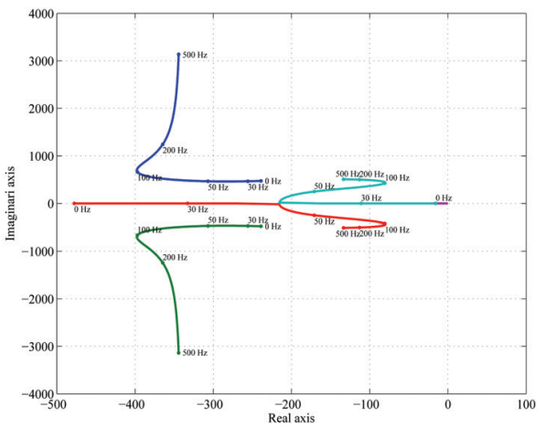

(a) Root locus of the system as a function of stator frequency when operating the motor at no-load

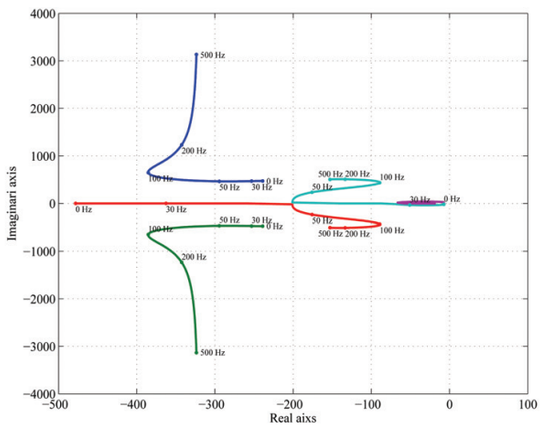

(b) Root locus of the system as a function of stator frequency when operating the motor at full-load

Fig. 1.10. Root locus of the stabilized motor as a function of stator frequency

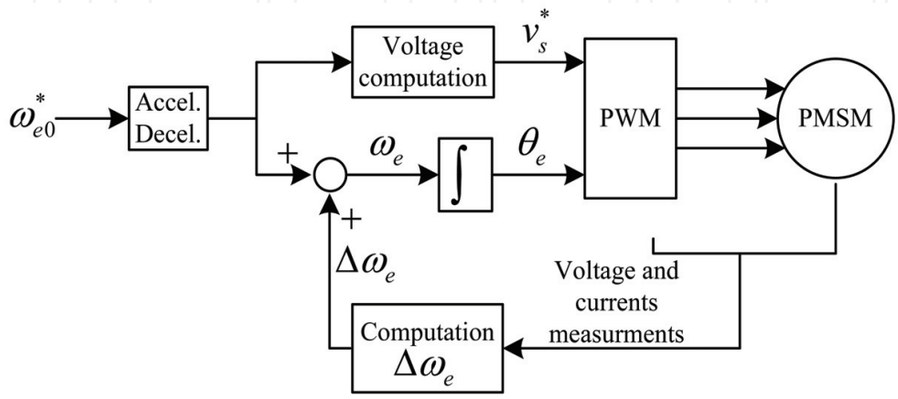

Fig. 1.11. Block diagram of the V/f control of PMSM with stabilization loop

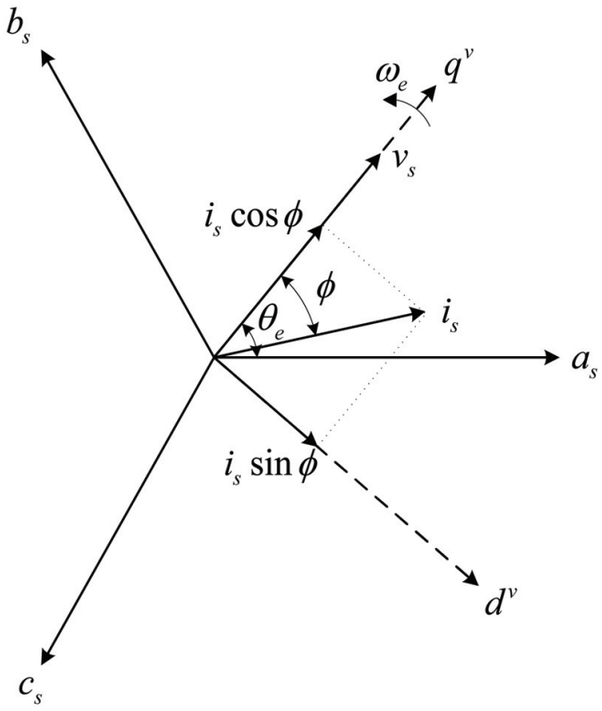

Fig. 1.12. Voltage and current vectors in the stator synchronous reference

5.1 Computation of power perturbations

The power delivered to the motor can be computed as

$$p_e = \frac{3}{2} v_s i_s \cos\phi \tag{1.33}$$

Observing Figure 1.12, $i_s \cos\phi$ can be computed as

$$i_{qs}^v = i_s \cos\phi = \frac{2}{3}\left(i_{as}\cos\theta_e + i_{bs}\cos\left(\theta_e - \frac{2\pi}{3}\right) - (i_{as}+i_{bs})\cos\left(\theta_e + \frac{2\pi}{3}\right)\right) \tag{1.34}$$

where the angle θ_e is the electrical angle of the applied voltage, and it is known. In (1.33), the v_s is the calculated voltage.

The input power perturbations can be easily obtained by a first order high-pass filter as

$$\Delta p_e = \frac{s}{s + \frac{1}{\tau_h}} p_e \tag{1.35}$$

5.2 Magnitude of the voltage vector

In the V/f control, the magnitude of the voltage vector is selected to maintain the motor flux constant, maintaining the relation V/f constant [13]. The steady state equations of the permanent magnet synchronous motor are

$$V_{ds}^r = R_s I_{ds}^r - \omega_{r0} L_q I_{qs}^r = R_s I_{ds}^r - \omega_{r0} \lambda_{ds}^r \tag{1.36}$$

$$V_{qs}^r = R_s I_{qs}^r + \omega_{r0} L_d I_{ds}^r + \omega_{r0} \lambda_m = R_s I_{qs}^r + \omega_{r0} \lambda_{qs}^r \tag{1.37}$$

If the resistive voltage droop is considered small

$$V_{ds}^r \approx -\omega_{r0} \lambda_{ds}^r \tag{1.38}$$

$$V_{qs}^r \approx \omega_{r0} \lambda_{qs}^r \tag{1.39}$$

The magnitude of the voltage vector is

$$V_s = \sqrt{\left(V_{ds}^r\right)^2 + \left(V_{qs}^r\right)^2} \approx \omega_{r0} \sqrt{\left(\lambda_{ds}^r\right)^2 + \left(\lambda_{qs}^r\right)^2} \tag{1.40}$$

and, then,

$$\frac{V_s}{\omega_{r0}} \approx \lambda_s \tag{1.41}$$

But, if the motor is operating at low speed or at high load level, the resistive voltage drop can not be neglected. When the motor operating at low speed or at high load level, maintaining the relation $\frac{V_s}{\omega_{r0}}$ constant does not maintains the flux constant, diminishing motor performance [14, 15]. In super-high-speed PMSM, with very low inductance, the stator resistance cannot be neglected even at high speeds [16]. Therefore, it is necessary to compensate the resistive voltage droop in the applied voltage. In HVAC applications, high-efficiency operation is desired. Low performance *V / f* control is ideal for efficiency-optimized control. This efficiency optimization can be achieved by means of controlling motor flux [17].

Voltage vector can be expressed adding the resistive voltage drop and the rotor permanent magnet induced voltage, as seen in Figure 1.13. The voltage vector can be expressed as

$$V_s = BC + CO = I_s R_s \cos\phi_0 + \sqrt{E_s^2 + I_s^2 R_s^2 \cos^2\phi_0 - I_s^2 R_s^2} \tag{1.42}$$

The vector E_s is the stator flux induced voltage. The stator flux is normally chosen to be equal as the rotor flux. Then,

$$E_s = \omega_{r0} \lambda_m \tag{1.43}$$

Even expression (1.42) is in steady state, the value of the voltage magnitude can be computed instantaneously as

$$v_s^* = R_s i_s \cos\phi + \sqrt{\left(\omega_{r0}\lambda_m\right)^2 + \left(R_s i_s \cos\phi\right)^2 - \left(R_s i_s\right)^2} \tag{1.44}$$

where i_s can be computed as

$$i_s = \sqrt{\left(i_{ds}^s\right)^2 + \left(i_{qs}^s\right)^2} = \sqrt{\frac{1}{3}\left(i_{as} + 2i_{bs}\right)^2 + \left(i_{as}\right)^2} \tag{1.45}$$

6. Experimental results

Figure 1.14 shows the block diagram of the implementation of the stabilizing loop. In i_s and $i_s \cos \phi$ computation, some ripple can be present. This ripple can affect the performance at low speed, deteriorating the voltage applied. Therefore, it is then necessary to filter these values. Figure 1.15 shows the variation of the variables in a no-load ramp up and then adding torque step change. As it can be seen, with the stabilizing loop, the motor operation is stable in the whole frequency range. Once the rated speed is reached, at time 4 s, a rated torque

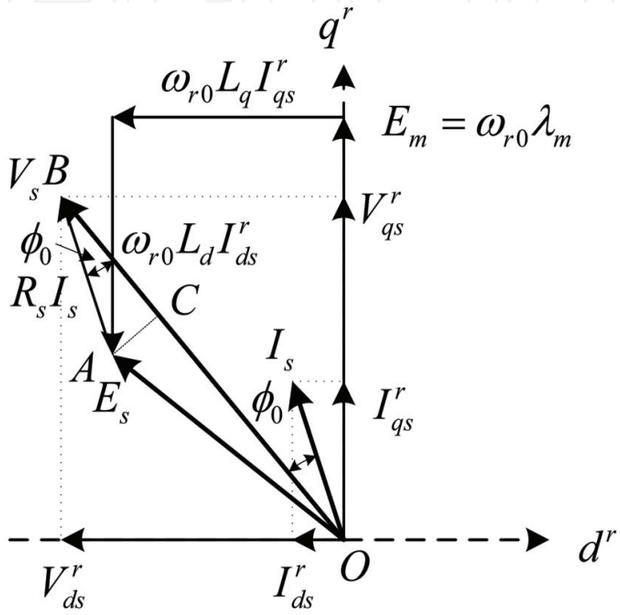

Fig. 1.13. Steady state vector diagram

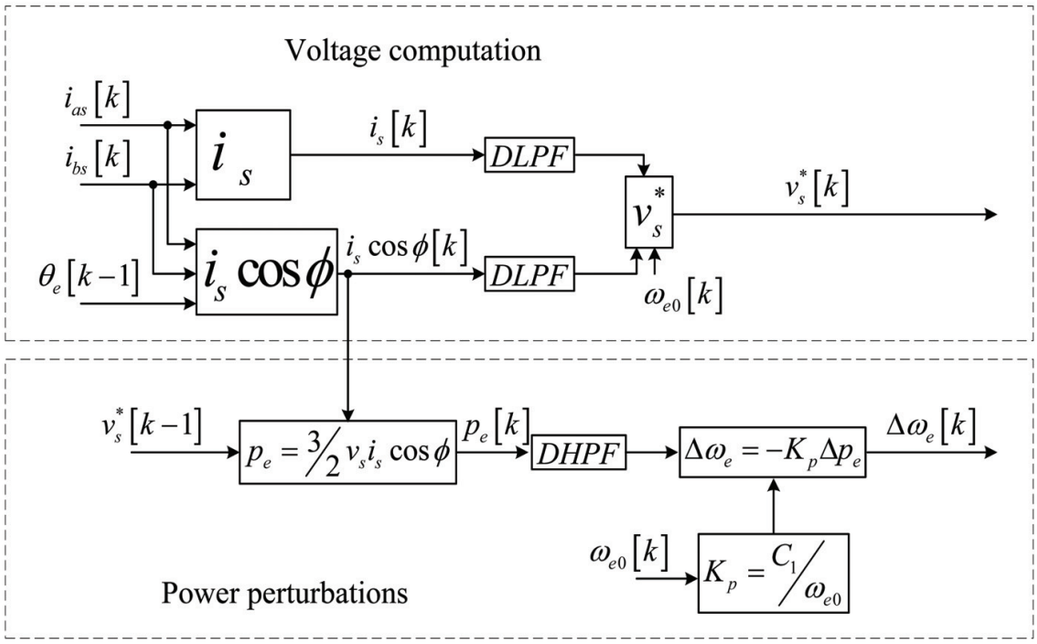

Fig. 1.14. Block diagram of the implementation of the stabilizing loop

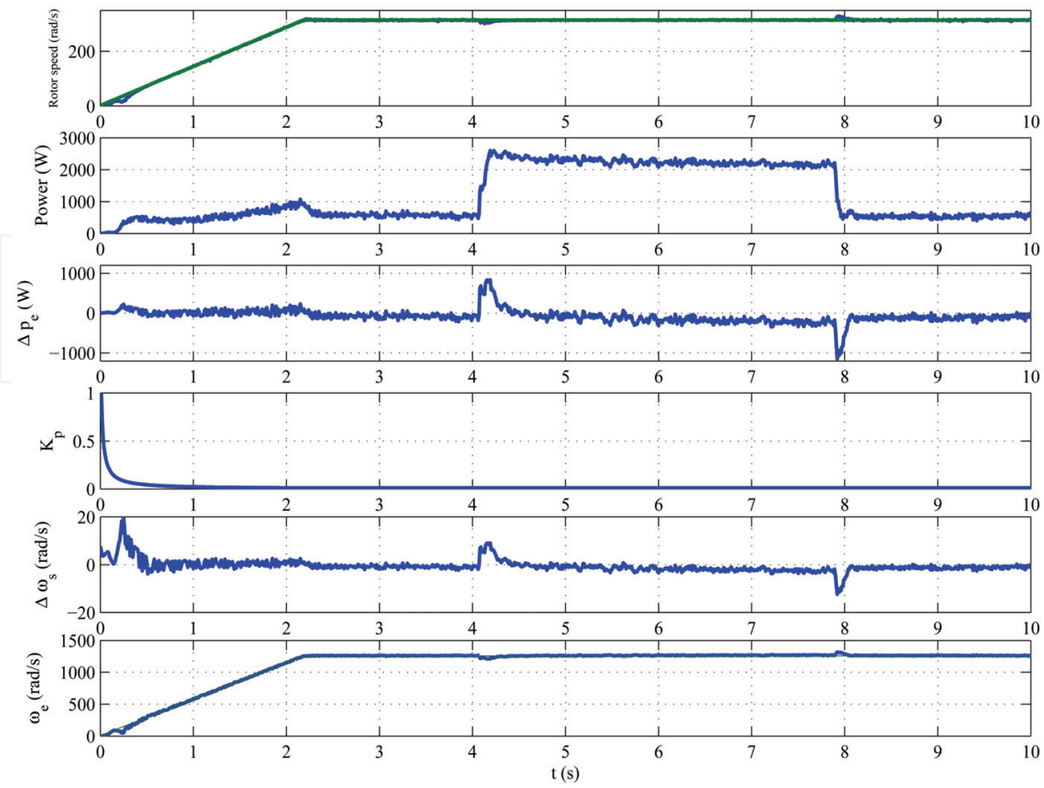

Fig. 1.15. Rotor speed, input power power perturbation, K_p, frequency perturbations $\Delta\omega_e$ and excitation frequency of the motor when operating at rated speed (200 Hz) with a load step.

step is applied, generating an input power perturbation. The stabilization loop compensates this perturbation, reducing the excitation frequency, and maintaining synchronism. At time 8 s, the torque is released, generating an input power perturbation. In this case, the stabilizing loop reacts increasing excitation frequency, to not to loose synchronization. In these torque steps, the variation of the rotation speed is less than 5 % of the rated speed during less than 200 ms. This performances are good enough for HVAC applications.

The variation of rotor speed when the stabilizing loop is removed can be seen in Figure 1.16. At time 7.5 s, the K_p is made zero, removing the stabilizing loop. Instantaneously, the motor loses synchronization.

The effects of the voltage vector resistive drop compensation can be seen in Figure 1.17. The motor is ramped up to a 40 Hz excitation frequency, including the resistive voltage drop compensation. Then, at time 7 s, this resistive voltage drop compensation is released, making R_s zero. Then voltage drop is no more compensated, and the motor loses synchronization, because not enough flux is created to maintain the rotor synchronized with the stator applied currents.

7. Conclusions

V/f control strategy for permanent magnet synchronous motors can be useful for HVAC applications, where not high performance is required. Permanent magnet synchronous motors have efficiency advantages over the induction motor. But open loop V/f control is not stable in the whole frequency range. As demonstrated, the V/f control strategy becomes

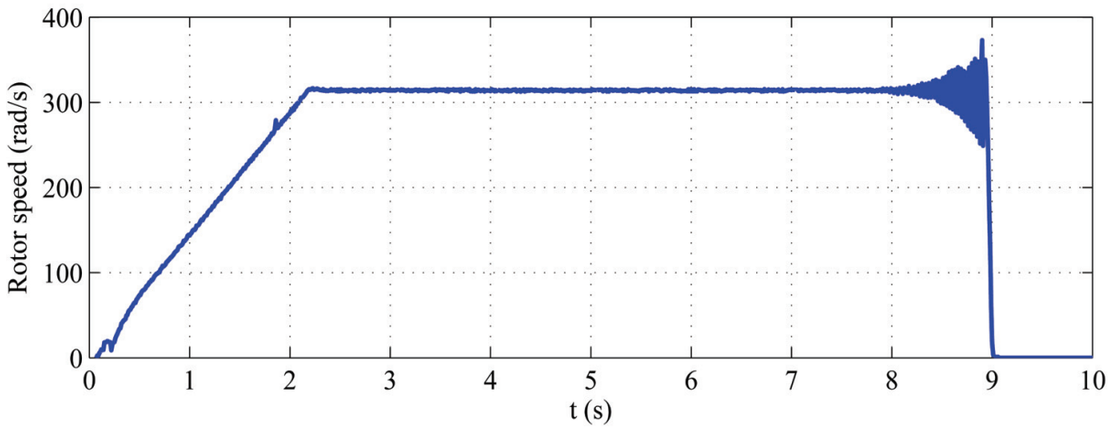

(a) Rotor speed

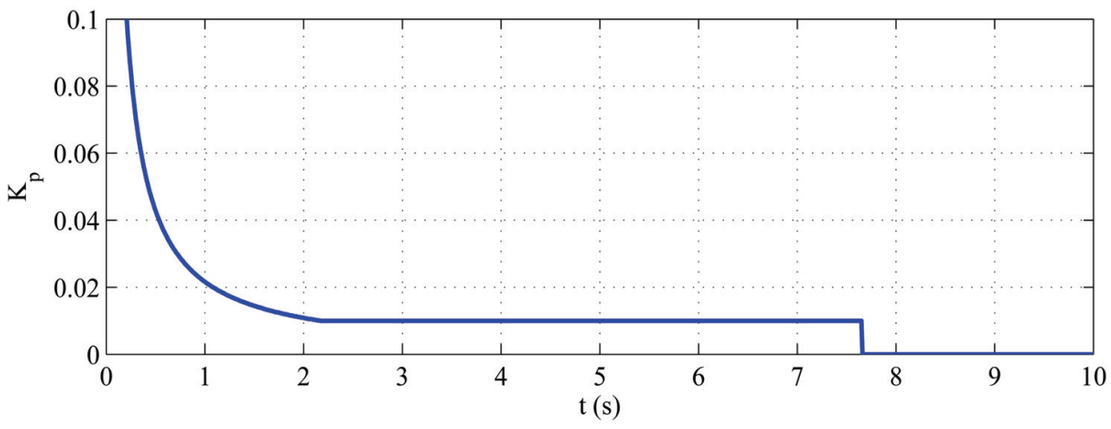

(b) K_p

Fig. 1.16. Rotor speed variation when $K_p = 0$

unstable, even at no-load, from a certain excitation frequency lower than the rated speed. Then, it is necessary to have a stabilizing loop in the system.

This stabilizing loop can be implemented by means of an speed measurement system, increasing cost, and complexity. The objective of this work is to develop a sensorless stabilizing loop. The presented strategy uses input power perturbations to stabilize the system. After adding the stabilizing loop, the V/f operation of the permanent magnet synchronous motor is stable for all the frequency range, and for any load torque applied to the motor.

Future research includes the estimation of the initial rotor position. Here, the motor is started from a known position, but for real applications, the rotor can be at any position. The stabilizing method developed uses some motor parameters. The variation of this parameters with temperature or even aging, must be studied. Increasing speed in PMSM over the rated speed means field weakening. For the operation above rated speed in HVAC applications is of interest, this method must be studied.

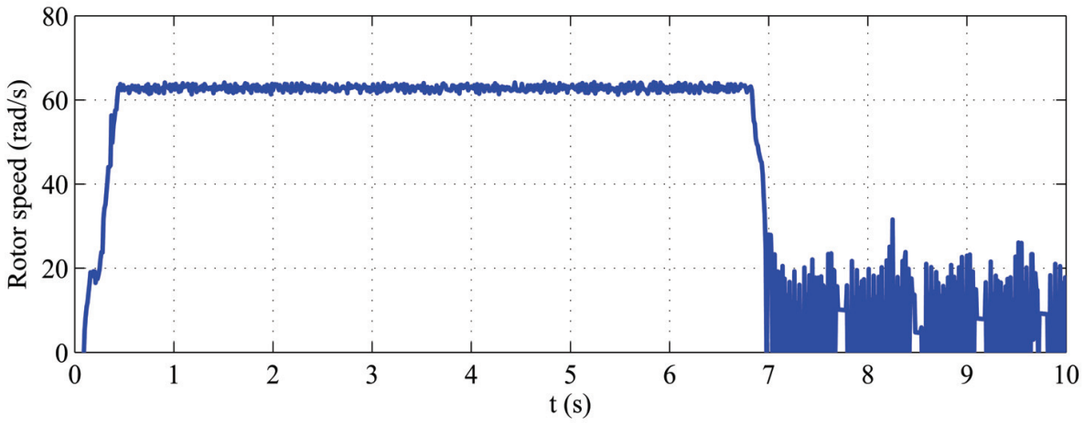

(a) Rotor speed at excitation frequency of 40 Hz

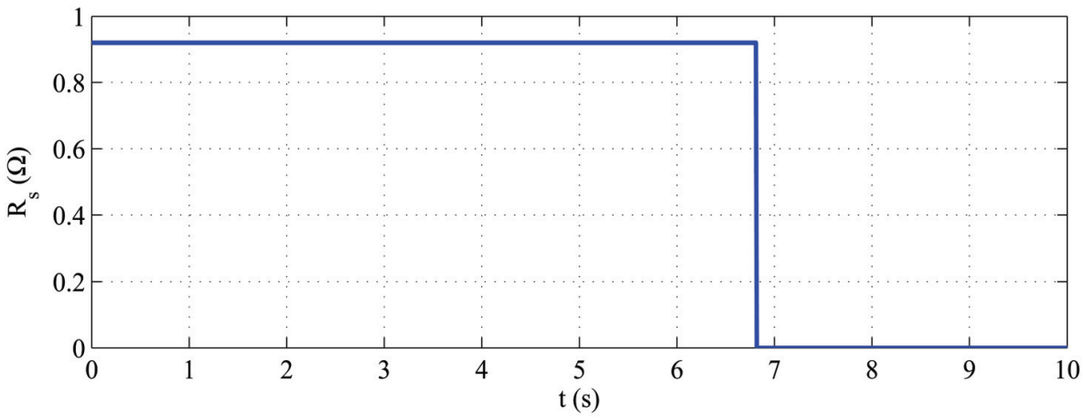

(b) R_s value used in computation. When it is made to zero, no voltage drop compensation is done

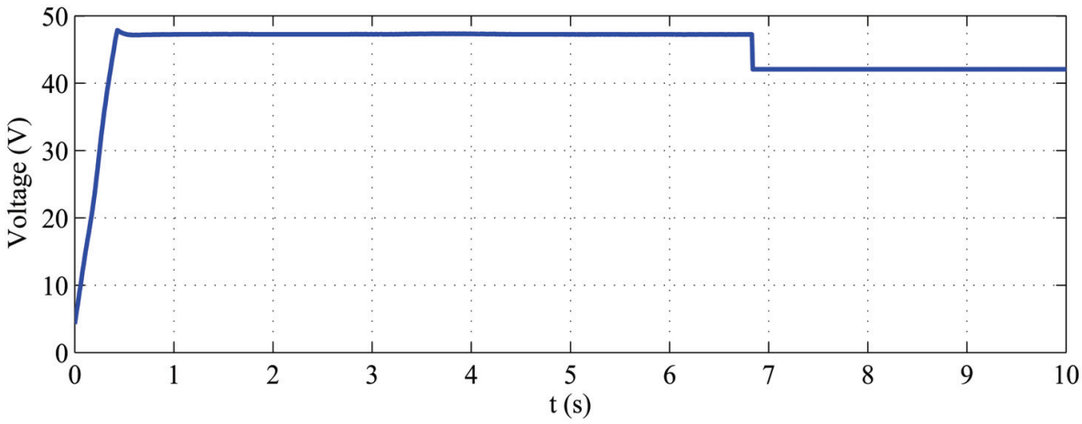

(c) Applied stator voltage

Fig. 1.17. Variation of rotor speed when there is no resistive voltage drop compensation at low speed (40 Hz)

A. Motor parameters

Model	MAVILOR BLS 115 4/400
Pole number (n)	8
Rated power	2,2 kW
Rated speed	3000 rpm
Rated frequency	200 Hz
Rated torque	8,1 Nm
Rated phase to phase voltage	400 V(rms)
Rated phase current	5,71 A(rms)
Stator resistance per phase (R_s)	0,92 Ω
d-axis inductance (L_d)	1,925 mH
q-axis inductance (L_q)	1,925 mH
Rotor permanent magnet flux (λ_m)	0,1674 V s rad^{-1}
Inertia of the mechanical system (J_m)	0,9724×10^{-3} kg m^2
Viscous friction coefficient (B_m)	1,3671×10^{-6} Nm s rad^{-1}

B. Linearization of the stabilized system

In order to analyze the stability of the system under frequency modulation, the model must be linearized. The linearized system has the form

$$\Delta \dot{x} = \mathbf{A}_1(\mathbf{X})\,\Delta \mathbf{x} + \mathbf{B}_1(\mathbf{X})\,\Delta T_l \tag{B.1}$$

where $\Delta\mathbf{x}$ is the state variables vector as

$$\Delta \mathbf{x} = \left\{ \Delta i_{ds}^r \quad \Delta i_{qs}^r \quad \Delta \omega_r \quad \Delta \delta \quad \Delta \omega_e \right\}^T \tag{B.2}$$

and the B_1 matrix is

$$\mathbf{B}_1(\mathbf{X}) = \begin{pmatrix} 0 & 0 & \frac{-n}{2J_m} & 0 & 0 \end{pmatrix}^T \tag{B.3}$$

The elements of the state matrix $\mathbf{A}_1$ are

$$A_{11} = -\frac{R_s}{L_d}, A_{12} = \frac{L_q \omega_{r0}}{L_d}, A_{13} = \frac{L_q I_{qs}^r}{L_d}, A_{14} = -\frac{V_s \cos\delta_0}{L_d}, A_{15} = 0$$

$$A_{21} = -\frac{L_d \omega_{r0}}{L_q}, A_{22} = -\frac{R_s}{L_q}, A_{23} = -\frac{1}{L_q}\left(L_d I_{ds}^r + \lambda_m\right), A_{24} = -\frac{V_s \sin\delta_0}{L_q}, A_{25} = 0$$

$$A_{31} = \frac{3}{2}\left(\frac{n}{2}\right)^2 \frac{1}{J_m}\left(L_d - L_q\right) I_{qs}^r, A_{32} = \frac{3}{2}\left(\frac{n}{2}\right)^2 \frac{1}{J_m}\left(\lambda_m + \left(L_d - L_q\right) I_{ds}^r\right),$$

$$A_{33} = -\frac{B_m}{J_m}, A_{34} = 0, A_{35} = 0$$

$$A_{41} = 0, A_{42} = 0, A_{43} = -1, A_{44} = 0, A_{45} = 1$$

$$A_{51} = \frac{3}{2}K_p V_s \left(\frac{L_d \omega_{r0} \cos\delta_0}{L_q} - \frac{R_s \sin\delta_0}{L_d} \right), A_{52} = \frac{3}{2}K_p V_s \left(\frac{R_s \cos\delta_0}{L_q} + \frac{L_q \omega_{r0} \sin\delta_0}{L_d} \right),$$

$$A_{53} = \frac{3}{2}K_p V_s \left(\left(\frac{L_q}{L_d} - 1 \right) I_{qs}^r \sin\delta_0 + \left(\left(\frac{L_d}{L_q} - 1 \right) I_{ds}^r + \frac{\lambda_m}{L_q} \right) \cos\delta_0 \right),$$

$$A_{54} = \frac{3}{2}K_p V_s \left(\left(\frac{1}{L_q} - \frac{1}{L_d} \right) V_s \sin 2\delta_0 + \frac{1}{L_d} \left(L_q \omega_{r0} I_{qs}^r - R_s I_{ds}^r \right) \cos\delta_0 - \right)$$
$$\left(\frac{1}{L_q} \left(R_s I_{qs}^r + \left(L_d I_{ds}^r + \lambda_m \right) \omega_{r0} \right) \sin\delta_0 \right),$$

$$A_{55} = \frac{3}{2}K_p V_s \left(I_{ds}^r \cos\delta_0 + I_{qs}^r \sin\delta_0 \right) - \frac{1}{\tau_h}$$

The eigenvalues of the state matrix can be used to analyze the stability characteristics of the system.

8. References

[1] P. Vas, Sensorless vector control and direct torque control. Oxford University Press, 1998.

[2] J. Itoh, N. Nomura, and hiroshi Ohsawa, "A comparison between *V/f* control and position-sensorless vector control for the permanent magnet synchronous motor," in *Proc. Power Conversion Conf.*, vol. 3, Osaka, Japan, Apr. 2002, pp. 1310-1315.

[3] P. D. Chandana Perera, "Sensorless control of permanent-magnet synchronous motor drives," Ph.D. dissertation, Institute of energy technology. Aalborg university, 2002.

[4] G. R. Slemon, *Electrical machines for drives*. IEEE Press, 1997, ch. 2 in Power electronics and variabale frequency drives. Tecnology and applications, pp. 36-76.

[5] T. M. Jahns, *Variable frequency permanent magnet AC machine drives*. IEEE Press, 1997, ch. 6 in Power electronics and variabale frequency drives. Tecnology and applications, pp. 277-325.

[6] B. K. Bose, Ed., Power electronics and variable frequency drives. Technology and applications. IEEE Press, 1997.

[7] D. W. Novotny and T. A. Lipo, *Vector control and dynamics of AC drives*, P. Hammond, T. J. E. Miller, and T. Kenjo, Eds. Oxford University Press, 2000.

[8] P. C. Krause, O. Wasynczuk, and S. D. Sudhoff, *Analysis of electrical machinery and drive systems*, 2nd ed. IEEE Press, 2002.

[9] G. C. Verghese, J. H. Lang, and L. F. Casey, "Analysis of instability in electrical machines," *IEEE Trans. Ind. Applicat.*, vol. IA-22, no. 5, pp. 853-864, 1986.

[10] R. S. Colby and D. W. Novotny, "An efficiency-optimizing permanent-magnet synchronous motor drive," *IEEE Trans. Ind. Applicat.*, vol. 24, no. 3, pp. 462-469, May/Jun. 1988.

[11] P. D. Chandana Perera, F. Blaabjerg, J. K. Pedersen, and P. Thøgersen, "A sensorless, stable *V/f* control method for permanent-magnet synchronous motor drives," *IEEE Trans. Ind. Applicat.*, vol. 39, no. 3, pp. 783-791, May/Jun. 2003.

[12] D. Montesinos-Miracle, "Modelització i control d'accionaments elèctrics," Ph.D. dissertation, Technical University of Catalonia, Jul. 2008.

[13] B. K. Bose, *Modern power electronics and AC drives*. Prentice Hall PTR, 2002.

[14] A. Munoz-Garcia, T. A. Lipo, and D. W. Novotny, "A new induction motor v/f control method capable of high-performance regulation at low speeds," *IEEE Trans. Ind. Applicat.*, vol. 34, no. 4, pp. 813-821, 1998.

[15] M. P. Kazmierkowski, R. Krishnan, and F. Blaabjerg, Eds., *Control in power electronics*, ser. Academic Press series in engineering. Academic Press. Elsevier Science, 2002.

[16] L. Zhao, C. H. Ham, Q. Han, T. X. Wu, L. Zheng, K. B. Sundaram, J. Kapat, and L. Chow, "Design of optimal digital controller for stable super-high-speed permanent-magnet synchronous motor," *IEE Proceedings -Electric Power Applications*, vol. 153, no. 2, pp. 213-218, 2006.

[17] F. Abrahamsen, F. Blaabjerg, J. K. Pedersen, and P. B. Thoegersen, "Efficiency-optimized control of medium-size induction motor drives," *IEEE Trans. Ind. Applicat.*, vol. 37, no. 6, pp. 1761-1767, 2001.

IntechOpen